This document is the accepted manuscript version of the following article:
Brumberg, A., Diroll, B. T., Nedelcu, G., Sykes, M. E., Liu, Y., Harvey, S. M., … Schaller, R. D. (2018). Material dimensionality effects on electron transfer rates between CsPbBr3 and CdSe nanoparticles. Nano Letters, 18(8), 4771-4776. https://doi.org/10.1021/acs.nanolett.8b01238

Material Dimensionality Effects on Electron Transfer Rates Between $CsPbBr_3$ and CdSe Nanoparticles

Alexandra Brumberg,[1] Benjamin T. Diroll,[2] Georgian Nedelcu,[3,4] Matthew E. Sykes,[2] Yuzi Liu,[2] Samantha M. Harvey,[1] Michael R. Wasielewski,[1] Maksym V. Kovalenko,[3,4] and Richard D. Schaller[1,2,*]

[1] Department of Chemistry, Northwestern University, 2145 Sheridan Rd, Evanston, IL 60208, USA

[2] Center for Nanoscale Materials, Argonne National Laboratory, 9700 Cass Ave, Lemont, IL, 60439, USA

[3] Department of Chemistry and Applied Biosciences, ETH Zürich, Vladimir-Prelog-Weg 1-5/10, CH-8093, Zürich, Switzerland

[4] Empa - Swiss Federal Laboratories for Materials Science and Technology, Überlandstrasse 129, CH-8600, Dübendorf, Switzerland

Abstract

Films containing mixtures of zero- or two-dimensional nanostructures (quantum dots or nanoplatelets) were prepared in order to investigate the impacts of dimensionality on electronic interactions. Electron transfer from $CsPbBr_3$ to CdSe was observed in all of the mixtures, regardless of particle dimensionality, and characterized via static and transient absorption and photoluminescence spectroscopies. We find that mixtures containing nanoplatelets as the electron acceptor (CdSe) undergo charge transfer more rapidly than those containing quantum dots. We believe the faster charge transfer observed with nanoplatelets may arise from the extended spatial area of the CdSe NPLs and/or the continuous density of acceptor states that are present in NPLs. These results bolster the use of one- or two-dimensional nanomaterials in the place of zero-dimensional quantum dots in the design of related optoelectronic devices such as solar cells, light-emitting diodes, and photocatalysts and further offer the prospect of fewer required hopping events to transport carriers due to the larger spatial extent of the particles.

Keywords: Nanoplatelets, electron transfer, dimensionality, perovskites, spectroscopy

Semiconductor nanoparticles (NPs) have been successfully implemented in numerous optoelectronic and photovoltaic applications, owing to synthetic control over the electronic structure via particle composition, size, and morphology. In many of these applications, NP shape has already been recognized as an additional way of optimizing functionality. For example, in quantum dot-sensitized solar cells, the use of higher dimensionality nanowires or rods in place of mesoporous TiO_2 or ZnO in solar cells results in improved electronic percolation throughout the cell,[1–4] while the use of CdSe nanorods as the sensitizing NP in place of spherical particles also leads to boosted performance.[5] Solar cells built on heterojunctions between CdSe and CdTe NPs or with CdSe/CdTe heterostructures have likewise shown that careful manipulation of size and shape offer routes toward augmenting charge transfer rates,[6,7] e.g. through the use of tetrapods or hyperbranched NPs.[8–10] NP morphology has also been explored as a method of maximizing carrier transport for photocatalysis through the use of nanorods, nanoplatelets, or various heterostructures.[11–14]

Colloidally-prepared, two-dimensional semiconductor nanoplatelets (NPLs) present a promising alternative to the zero-dimensional quantum dots (QDs) that are used in the aforementioned applications, owing to strong light absorption and the possibility of rapid charge transfer. NPLs are well-suited to function as light absorbers or emitters since large total volumes result in large per-particle absorption cross-sections that are typically an order of magnitude greater than those of QDs,[15–17] while near-zero dispersity of NPL thickness leads to narrow band-edge absorption and emission that can be tuned synthetically.[18–20] Both $CsPbBr_3$ and CdSe can be synthesized as NPLs,[18,21,22] presenting an appropriate system in which to study the effect of dimensionality on electronic interactions. Moreover, $CsPbBr_3$ has recently received significant

attention both in optoelectronic and photovoltaic applications,[23–26] while CdSe represents a well-studied material for which it is possible to synthesize QDs and NPLs of not just the same crystal structure, but also the same band gap. Furthermore, studies of CdSe NPLs have shown that these structures exhibit faster rates of energy transfer between disparate particles than QDs.[27] Fast rates were attributed to large space filling of acceptor in proximity to donor, and similar considerations could suggest that charge transfer may likewise occur more rapidly between NPLs.

For molecular systems, Marcus theory provides a description of the rate of electron transfer between two molecules as a function of separation distance and driving force.[28] While driving force remains straightforward to calculate for NP systems, other parameters—such as distance—are more complex, raising the question of whether a standard form of Marcus theory remains valid for systems comprised of spatially extended NPs. Others have pursued this question in QD-donor and molecular-acceptor systems by investigating the dependence of the electron transfer rate on distance and driving force.[29–32] Owing to these studies, an analogous formulation of Marcus theory for QDs with strongly bound acceptors has been reported, in which electron transfer is accompanied by hole excitation in the donor.[31,33,34] On the other hand, more recent studies of charge transfer in systems in which both the electron donor and the electron acceptor are comprised of QDs suggest that Marcus theory is still valid provided that the final electronic states are summed over.[35] While both approaches relate that Marcus theory necessitates modification when describing charge transfer to or from a NP, they do not contemplate the additional factor of NP shape (dimension), which must be considered to relate rates of electron transfer for NPs of the same energetics but different physical extent.

Evaluating the role of dimensionality is complicated by the need to control for factors that could result in differing rates of electron transfer, independent of the particle shape. Fortunately, for some materials it is possible to synthesize NPs of different shapes or dimensions (such as zero-dimensional QDs and two-dimensional NPLs) yet isoenergetic band gaps, allowing for the charge transfer driving force to be kept constant. For example, studies looking at the effect of lateral area of NPLs[36] or aspect ratio of nanorods[37] on charge transfer to a molecular acceptor have successfully compared rates between particles of varying sizes and nearly isoenergetic band gaps. Distance is a more difficult factor to control when the acceptor is not chemically bound to the donor, although the use of identical surface ligands can accomplish such a task.

In this work, we investigate electronic interactions between $CsPbBr_3$ and CdSe NPs to determine the impact of NP dimensionality on charge transfer rates. Zero- and two-dimensional NPs of both $CsPbBr_3$ and CdSe are studied so as to compare electronic interactions between 0D-0D, 0D-2D, and 2D-2D systems. Electron transfer is observed via transient absorption (TA) and static and time-resolved photoluminescence (PL and trPL) measurements. Electron transfer rates are extracted from time-resolved dynamics and become faster in systems containing 2D NPs

versus systems with 0D NPs, relaying a potential benefit of spatially extended structures in derived optoelectronics.

The absorption and emission spectra of the CdSe and $CsPbBr_3$ QDs and NPLs used in this work appear in Figure 1A. Notably, the examined zinc-blende CdSe QDs and NPLs exhibit nearly isoenergetic emission maxima at 546 nm and 555 nm, respectively, placing the difference in their band gaps at approximately 37 meV—only moderately larger than thermal energy at room temperature (26 meV). As shown in Figure 1B, the particles present quite different shapes and sizes. The CdSe QDs are roughly 3 nm in diameter,[38] whereas the 5-monolayer CdSe NPLs are 1.5 nm thick and tens of nanometers along each side laterally. The examined $CsPbBr_3$ QDs are roughly 8 nm on each side with a nearly cubic morphology,[39] similar to the side lengths of 10-11 nm and 12-14 nm of the $CsPbBr_3$ NPLs but larger than the 3-4 nm thickness.

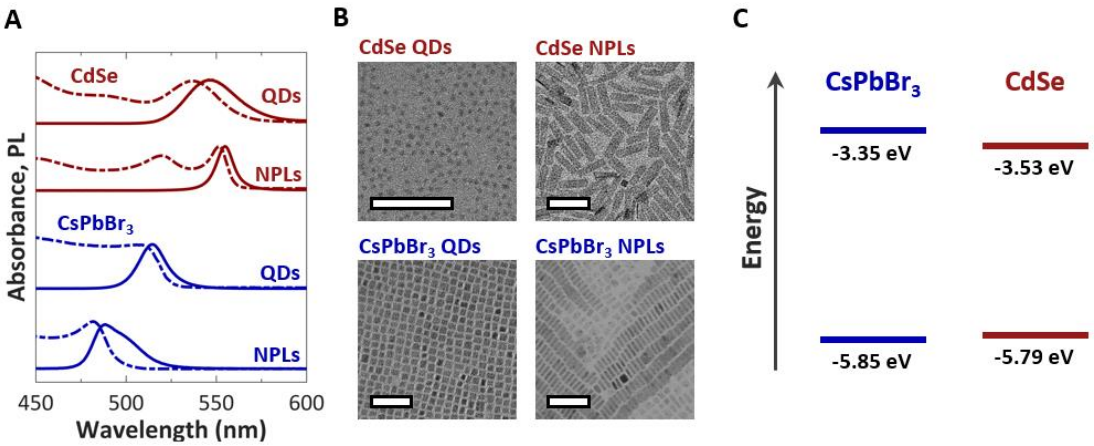

Figure 1. (A) Normalized solution absorption (dashed lines) and film photoluminescence (solid lines) spectra, offset vertically for clarity, and **(B)** TEM images of CdSe QDs and NPLs and $CsPbBr_3$ QDs and NPLs. TEM scale bars are 50 nm. **(C)** Conduction and valence band levels of $CsPbBr_3$ QDs and CdSe NPLs, based on values reported in Refs. 43 and 45. Although the exact energies vary for QDs and NPLs of each material, electron transfer is energetically favorable for each combination of $CsPbBr_3$ and CdSe.

Stock solutions of either $CsPbBr_3$ or CdSe NPs in hexane were mixed in controlled ratios by concentration (i.e. particle number; see the SI for details) and then drop-casted where solvent rapidly evaporated; the ratios spanned the range of dilute to concentrated amounts of one in the other to explore the additive kinetics of the electronic interactions. When $CsPbBr_3$ and CdSe NPs are mixed, substantive regions of mixed particles do form (see Figure S1). We note this since reports show that disparate particle types can, under some conditions, resist mixing in attempts at forming ordered binary superlattices,[40–42] which are not pursued here. In mixed particle films where different particle types can surround one another, electron transfer (ET) and fluorescence resonance energy transfer (FRET) may occur. As shown in Figure 1C, ET is possible, as the measured conduction band (CB) of $CsPbBr_3$ is more reducing than that of CdSe by ~50 to 150

meV.[43–45] FRET from $CsPbBr_3$ to CdSe is also possible, as $CsPbBr_3$ emission overlaps with CdSe absorption (see Figure 1A).

The dynamics of the dropcast films were probed using low fluence 400 nm excitation so as to avoid multiexcitonic processes (see the SI for details). Figure 2A shows the TA dynamics of the CdSe NPL absorption bleach that appears at 551 nm, arising from state-filling of the conduction band.[46] For a neat CdSe NPL film, the bleach decays slowly over a 1 ns time window, conveying a loss of conduction band electrons through recombination. Conversely, a distinct rise of the CdSe bleach occurs for a mixed film containing 95% $CsPbBr_3$ QDs and 5% CdSe NPLs. Since pure $CsPbBr_3$ lacks spectral signatures near 551 nm (TA spectra of neat CdSe and $CsPbBr_3$ films appear in Figure S2), the rise of the 551 nm bleach relates a clearly *increasing* population of electrons in the CdSe conduction band. The differing dynamics of the pure and mixed films are also apparent from time-resolved spectra presented in Figure 2B.

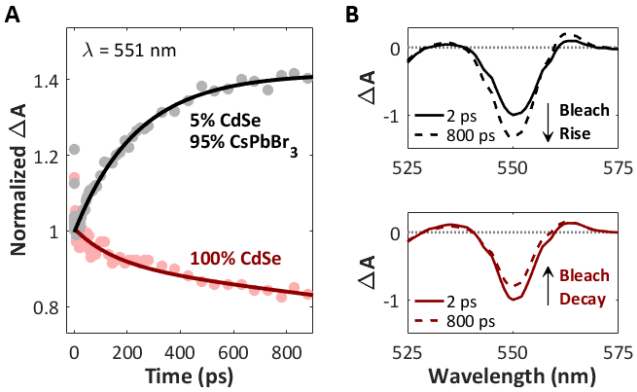

Figure 2. Evidence for an influx of electrons into CdSe NPLs from $CsPbBr_3$ QDs through transient absorption (TA). **(A)** TA dynamics of the CdSe NPL bleach (monitored at 551 nm) in films excited at 400 nm. While the bleach of the CdSe film decays over time, the decay in a film with both CdSe NPLs and $CsPbBr_3$ QDs slows down as the fraction of $CsPbBr_3$ is increased until a rise in the bleach is seen instead for films of 5% CdSe and 95% $CsPbBr_3$. Solid lines are exponential fits to the data. **(B)** TA spectra of the same films as in (A) at 2 ps (solid lines) and 800 ps (dashed lines).

With increasing CdSe NPL fraction, more instances of electron or energy transfer from $CsPbBr_3$ to CdSe can occur, since the latter acts as an acceptor for each process. To gain more insight as to which process dominates, we investigated photoluminescence properties. Figure 3A shows static PL spectra of a neat $CsPbBr_3$ QD film and mixed films containing 95%, 85%, or 35% $CsPbBr_3$, excited at 405 nm. A nearly complete drop of PL intensity is observed for films containing 85% $CsPbBr_3$ QDs (15% CdSe NPLs). Furthermore, Figure 3B displays a nonlinear drop in integrated $CsPbBr_3$ PL intensity as the mole fraction of $CsPbBr_3$ is decreased (CdSe fraction increased). Together, the panels in Figure 3 demonstrate that either electron transfer or FRET successfully quenches $CsPbBr_3$ emission in mixed films. Photoluminescence excitation

(PLE) was performed to evaluate whether electron transfer, FRET, or both represent a main pathway through which electrons are transferred to CdSe. PLE spectra of mixed films (presented in Figure S3) do not show increased CdSe emission for excitation wavelengths where $CsPbBr_3$ is excited, indicating that $CsPbBr_3$ does not undergo energy transfer to CdSe after photoexcitation with appreciable efficiency. This suggests that the rising CdSe TA signals with time and the quenched PL of $CsPbBr_3$ result from electron transfer.

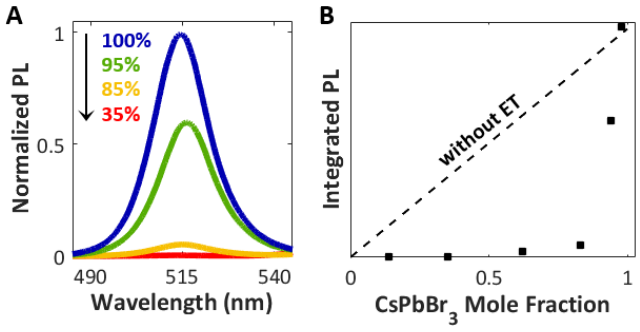

Figure 3. Evidence for an influx of electrons into CdSe NPLs from $CsPbBr_3$ QDs through static PL. **(A)** Static PL spectra of films of $CsPbBr_3$ QDs and CdSe NPLs, normalized by the absorption of each film at the excitation wavelength of 405 nm. The percentages indicate the fraction of $CsPbBr_3$ in each film. As the fraction of $CsPbBr_3$ is decreased and the corresponding fraction of CdSe is increased, the PL of $CsPbBr_3$ is drastically quenched, much more than would be expected by the reduced fraction of $CsPbBr_3$. **(B)** The integrated PL intensity of the $CsPbBr_3$ emission shown in (A), as compared to the intensity that would be expected for each film based on its fraction of $CsPbBr_3$ in the absence of any electron or energy transfer.

Time-resolved PL at low fluence further supports dominance of electron transfer in this mixed system. Figure 4 shows trPL of the $CsPbBr_3$ component, which becomes shorter-lived in mixed films, indicating outflow of electrons from $CsPbBr_3$ into CdSe. Notably, trPL of the CdSe component (shown in Figure S4) does not exhibit the slowed PL decay or rise in intensity with time that would be expected if energy transfer were providing CdSe with additional excitons that could radiatively recombine. This corroborates PLE in suggesting that electron transfer constitutes the dominant pathway of electronic interaction between $CsPbBr_3$ and CdSe NPs.

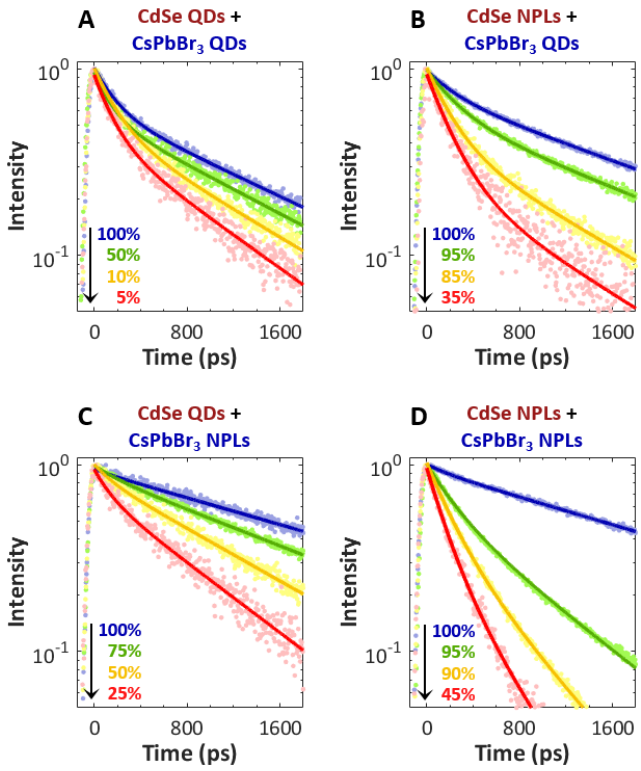

Figure 4. Time-resolved PL decay dynamics of the $CsPbBr_3$ emission in mixes of **(A, C)** CdSe QDs or **(B, D)** CdSe NPLs mixed with either **(A, B)** $CsPbBr_3$ QDs or **(C, D)** $CsPbBr_3$ NPLs. As the fraction of $CsPbBr_3$ is decreased and the fraction of CdSe is increased, the PL decay of the $CsPbBr_3$ emission gets faster. In the mixes containing CdSe QDs, the amount of CdSe required to see fast PL decay is much higher compared to the films containing CdSe NPLs. Solid lines are biexponential fits to the data.

The multiple panels in Figure 4 correspond to trPL of $CsPbBr_3$ for four series of films comparing particle dimensionality (CdSe QDs or NPLs mixed with either $CsPbBr_3$ QDs or NPLs). All four sets of films relate increasing rates of electron transfer as the CdSe particle fraction is increased, as expected from the additive kinetics of electron transfer. However, much higher amounts of CdSe QDs are needed in order to observe significant differences in the PL decay as compared to CdSe NPLs. For example, in films containing $CsPbBr_3$ NPLs and CdSe NPLs (Figure 4D), even with only 5% CdSe, a substantial drop in PL intensity (corresponding to much faster PL decay and electron transfer) is observed. Conversely, in films containing $CsPbBr_3$ QDs and CdSe QDs (Figure 4A), even when the film is 95% CdSe, the drop in PL intensity is comparatively small.

Because the driving force for charge transfer in films containing $CsPbBr_3$ QDs versus those containing $CsPbBr_3$ NPLs is not identical in the present measurements, the most direct comparisons that can be made are for films composed of the fixed types of $CsPbBr_3$ particles. Figures 4A and 4B compare CdSe QDs versus CdSe NPLs for films containing $CsPbBr_3$ QDs, and Figures 4C and 4D make the same comparison for films containing $CsPbBr_3$ NPLs. In both

cases, it is apparent that CdSe NPLs function as higher efficiency electron acceptors. Since the band gaps of CdSe QDs and NPLs are approximately isoenergetic, the driving force for charge transfer is fixed and does not contribute differences in the observed dynamics, which instead suggests that the disparity of response arises from particle dimensionality. Additional observations in support of this statement are derived from experiments repeated with larger CdSe QDs that absorb near 553 nm and emit near 586 nm, placing the difference in driving force between these CdSe QDs and the CdSe NPLs (calculated from the difference in their emission energies) at 118 meV. Figure S5 suggests that electron transfer rates are still slow, even though CdSe QDs with a much larger driving force for electron transfer from $CsPbBr_3$ in comparison to the examined CdSe NPLs are employed.

To quantify the observed differences in rates, the $CsPbBr_3$ trPL decay dynamics for each film are fit to biexponential decays, and an amplitude-weighted average lifetime is calculated. In a mixed film containing both $CsPbBr_3$ and CdSe particles, PL decay in $CsPbBr_3$ arises both from the decay processes that occur in pure $CsPbBr_3$ and owing to electron transfer to CdSe. The rate of PL decay in the mixed film can therefore be expressed as:

$$k_{\mathrm{mix}} = (1-x)k_{\mathrm{CsPbBr_3}} + xk_{\mathrm{ET}} \#(1)$$

such that

$$k_{\mathrm{ET}} = \frac{k_{\mathrm{mix}} - (1-x)k_{\mathrm{CsPbBr_3}}}{x} \#(2)$$

where $\langle\tau\rangle_{\mathrm{mix}} = 1/k_{\mathrm{mix}}$ and $\langle\tau\rangle_{\mathrm{CsPbBr_3}} = 1/k_{\mathrm{CsPbBr_3}}$ are the amplitude-weighted $CsPbBr_3$ emission lifetimes of the mixed and pure films, respectively, k_{ET} is the rate of electron transfer, and x is the fraction of $CsPbBr_3$ particles in the film that undergo electron transfer. Here, x is calculated by assuming that any decrease in intensity at long times (i.e. 1.8 ns, significantly later than the sub-nanosecond timescale on which electron transfer occurs) beyond that of the neat film must stem from electron transfer that occurred prior, since decay at long times is governed by that of neat $CsPbBr_3$. As such, the ratio of intensities at long times for the film containing both $CsPbBr_3$ and CdSe in comparison to the pure $CsPbBr_3$ film gives the fraction of $CsPbBr_3$ particles that did not undergo electron transfer, $1-x$, from which x can be determined.

Table 1 provides the rates of electron transfer for each film obtained from fitting the trPL decays shown in Figure 4. (Table S3 in the SI contains the amplitude-weighted lifetimes and the fractions of $CsPbBr_3$ particles that undergo electron transfer in each film.) Films with either CdSe QDs or NPLs and the same type of $CsPbBr_3$ NPs, such as QDs, can be compared directly to determine what effect dimensionality plays on the rates of electron transfer. The corresponding columns in Table 1 show that for equivalent fractions of CdSe, films containing CdSe NPLs exhibit faster rates of electron transfer.

Table 1. Electron transfer rates k_{ET} from $CsPbBr_3$ to CdSe as a function of CdSe fraction.

CdSe Fraction	k_{ET} (ps^{-1}) in films with:			
	CdSe QDs / $CsPbBr_3$ QDs	CdSe NPLs / $CsPbBr_3$ QDs	CdSe QDs / $CsPbBr_3$ NPL	CdSe NPLs / $CsPbBr_3$ NPLs
10%	-	$1.4\pm0.2 \times 10^{-3}$	$1.1\pm0.2 \times 10^{-3}$	$1.9\pm0.1 \times 10^{-3}$
15 - 25%	-	$2.1\pm0.2 \times 10^{-3}$	$1.2\pm0.1 \times 10^{-3}$	$2.8\pm0.3 \times 10^{-3}$
40 - 55%	$1.9\pm0.4 \times 10^{-3}$	$2.2\pm0.2 \times 10^{-3}$	$1.4\pm0.1 \times 10^{-3}$	$3.8\pm0.6 \times 10^{-3}$
75 - 85%	$2.2\pm0.3 \times 10^{-3}$	$3.3\pm0.8 \times 10^{-3}$	$1.7\pm0.2 \times 10^{-3}$	$5.7\pm0.9 \times 10^{-3}$
90%	$2.2\pm0.3 \times 10^{-3}$	-	$1.7\pm0.5 \times 10^{-3}$	-

Table 1 shows rates of electron transfer from $CsPbBr_3$ increase with increasing amounts of CdSe (again for low pump fluence), as would be expected for additive kinetics. Here, the ratio of donor to acceptor in each film was varied in an attempt to pursue characterization of the fundamental bimolecular rate constant, which describes the rate of electron transfer in the limit of one acceptor per donor. In randomly mixed films, such a situation is difficult to orchestrate, as demonstrated by Figure S1; despite mixing of acceptor and donor, the two do not evenly disperse in one another. Regardless, the asymptotic limit of such behavior likely relates the bimolecular limit. The case of small fraction of CdSe in $CsPbBr_3$ can parallel the limit in which a bimolecular rate constant can be obtained; however, the situation is complicated by the fact that electron transfer is not distinctly observable for especially dilute amounts of CdSe QDs in $CsPbBr_3$ QDs.

Faster rates of electron transfer in systems containing 2D materials versus their 0D counterparts can perhaps be understood by considering the larger spatial extent of the 2D NPLs versus the 0D QDs. The greater NPL surface area per particle presents more opportunities for electron transfer, similar to additive kinetics of discrete electron acceptors.[36,47] Such increased spatial extent facilitates faster rates of FRET,[27] owing to the increase in the number of nearest neighbors that is afforded by the extended area of the NPL. Additionally, the 2D NPLs present a continuous density of acceptor states, whereas the 0D QD acceptors offer discretized energy levels. The continuous density of states of the NPLs offer more opportunities for electron transfer, each with a distinct free energy change. These states are then integrated over in the kinetics of electron transfer and can facilitate an increased overall rate of electron transfer relative to QD acceptors.

Given that the faster rates of charge transfer in systems containing NPLs likely arise from the extended spatial areas of the NPLs, it is probably true that the orientations of the acceptor CdSe NPLs relative to the $CsPbBr_3$ donors influence the rate of charge transfer, particularly in the case of $CsPbBr_3$ NPL donors. The fastest rate would be expected for cofacial arrangements of $CsPbBr_3$ NPLs and CdSe NPLs, such that the opportunities for electron transfer are optimized. A similar argument is presented in Rowland *et al.* for energy transfer between cofacially stacked

CdSe NPLs. Future work could benefit from synthetic routes to cofacial arrangements, as well as theoretical analysis of different QD and NPL configurations, as the geometry of each particle is certain to influence the observed electron transfer rate.

In conclusion, we have identified electron transfer in mixed films of $CsPbBr_3$ and CdSe using static and time-resolved photoluminescence and transient absorption spectroscopies. Rates of electron transfer in films containing different types of $CsPbBr_3$ and CdSe NPs are extracted from trPL decays and show that electron transfer is faster for 2D materials such as NPLs than it is for 0D materials such as QDs. These findings offer potential implications in the design of solar cells or other devices in which it is critical to maximize rates of charge transfer.

ASSOCIATED CONTENT

Supporting Information. Experimental methods (synthesis of NPs, film preparation, and spectroscopic measurements), calculation of $CsPbBr_3$ and CdSe stock solution concentrations, verification of the single exciton excitation regime, transient absorption spectra of pure $CsPbBr_3$ and CdSe, photoluminescence excitation spectra, time-resolved photoluminescence of the CdSe component, photoluminescence data analysis methods, time-resolved photoluminescence data fits, electron transfer with higher energy CdSe QDs, and TEM images of films containing both $CsPbBr_3$ and CdSe. (PDF)

AUTHOR INFORMATION

Corresponding Author

* schaller@anl.gov

Notes

The authors declare no competing financial interest.

ACKNOWLEDGMENTS

This material is based upon work supported by the National Science Foundation under Grant No. DMREF-1629383 (A.B., B.T.D., S.M.H., R.D.S.), the National Science Foundation Graduate Research Fellowship Program under Grant No. DGE-1324585 (A.B.), the Chemical Sciences, Geosciences, and Biosciences Division, Office of Basic Energy Sciences, DOE under Grant DE-FG02-99ER14999 (S.M.H., M.R.W.), the European Union through the FP7 (ERC Starting Grant NANOSOLID, GA No. 306733) (G.N., M.V.K.), and the Swiss Federal Commission for Technology and Innovation (CTI-No. 18614.1 PFNM-NM) (G.N., M.V.K.). Use of the Center for Nanoscale Materials, an Office of Science user facility, was supported by the U.S. Department of Energy, Office of Science, Office of Basic Energy Sciences, under Contract No. DE-AC02-06CH11357. G.N. and M.V.K. acknowledge the support of the Scientific Center for Optical and Electron Microscopy (ETH Zürich).

References

(1) Benkstein, K. D.; Kopidakis, N.; van de Lagemaat, J.; Frank, A. J. *J. Phys. Chem. B* **2003**, *107*, 7759–7767.

(2) Law, M.; Greene, L. E.; Johnson, J. C.; Saykally, R.; Yang, P. *Nat. Mater.* **2005**, *4*, 455–459.

(3) Mor, G. K.; Shankar, K.; Paulose, M.; Varghese, O. K.; Grimes, C. A. *Nano Lett.* **2006**, *6*, 215–218.

(4) Kongkanand, A.; Tvrdy, K.; Takechi, K.; Kuno, M.; Kamat, P. V. *J. Am. Chem. Soc.* **2008**, *130*, 4007–4015.

(5) Salant, A.; Shalom, M.; Tachan, Z.; Buhbut, S.; Zaban, A.; Banin, U. *Nano Lett.* **2012**, *12*, 2095–2100.

(6) Gur, I.; Fromer, N. A.; Geier, M. L.; Alivisatos, A. P. *Science* **2005**, *310*, 462–465.

(7) Liu, R.; Bloom, B. P.; Waldeck, D. H.; Zhang, P.; Beratan, D. N. *J. Phys. Chem. C* **2017**, *121*, 14401–14412.

(8) Milliron, D.; Hughes, S. M.; Cui, Y.; Manna, L.; Li, J.; Wang, L. W.; Alivisatos, A. P. *Nature* **2004**, *430*, 190–195.

(9) Milliron, D. J.; Gur, I.; Alivisatos, A. P. *MRS Bull.* **2005**, *30*, 41–44.

(10) Gur, I.; Fromer, N. A.; Chen, C. P.; Kanaras, A. G.; Alivisatos, A. P. *Nano Lett.* **2007**, *7*, 409–414.

(11) Zhu, H.; Song, N.; Lv, H.; Hill, C. L.; Lian, T. *J. Am. Chem. Soc.* **2012**, *134*, 11701–11708.

(12) Sitt, A.; Hadar, I.; Banin, U. *Nano Today* **2013**, *8*, 494–513.

(13) Elmalem, E.; Saunders, A. E.; Costi, R.; Salant, A.; Banin, U. *Adv. Mater.* **2008**, *20*, 4312–4317.

(14) Zhukovskyi, M.; Tongying, P.; Yashan, H.; Wang, Y.; Kuno, M. *ACS Catal.* **2015**, *5*, 6615–6623.

(15) Yeltik, A.; Delikanli, S.; Olutas, M.; Kelestemur, Y.; Guzelturk, B.; Demir, H. V. *J. Phys. Chem. C* **2015**, *119*, 26768–26775.

(16) Kunneman, L. T.; Tessier, M. D.; Heuclin, H.; Dubertret, B.; Aulin, Y. V; Grozema, F. C.; Schins, J. M.; Siebbeles, L. D. A. *J. Phys. Chem. Lett.* **2013**, *4*, 3574–3578.

(17) She, C. X.; Fedin, I.; Dolzhnikov, D. S.; Demortiere, A.; Schaller, R. D.; Pelton, M.; Talapin, D. V. *Nano Lett.* **2014**, *14*, 2772–2777.

(18) Ithurria, S.; Tessier, M. D.; Mahler, B.; Lobo, R. P. S. M.; Dubertret, B.; Efros, A. L. *Nat. Mater.* **2011**, *10*, 936–941.

(19) She, C.; Fedin, I.; Dolzhnikov, D. S.; Dahlberg, P. D.; Engel, G. S.; Schaller, R. D.; Talapin, D. V. *ACS Nano* **2015**, *9*, 9475–9485.

(20) Tessier, M. D.; Javaux, C.; Maksimovic, I.; Loriette, V.; Dubertret, B. *ACS Nano* **2012**, *6*, 6751–6758.

(21) Bekenstein, Y.; Koscher, B. A.; Eaton, S. W.; Yang, P.; Alivisatos, A. P. *J. Am. Chem. Soc.* **2015**, *137*, 16008–16011.

(22) Ithurria, S.; Dubertret, B. *J. Am. Chem. Soc.* **2008**, *130*, 16504–16505.

(23) Swarnkar, A.; Chulliyil, R.; Ravi, V. K.; Irfanullah, M.; Chowdhury, A.; Nag, A. *Angew. Chemie - Int. Ed.* **2015**, *127*, 15644–15648.

(24) Li, J.; Xu, L.; Wang, T.; Song, J.; Chen, J.; Xue, J.; Dong, Y.; Cai, B.; Shan, Q.; Han, B.; et al. *Adv. Mater.* **2017**, *29*, 1603885.

(25) Kulbak, M.; Cahen, D.; Hodes, G. *J. Phys. Chem. Lett.* **2015**, *6*, 2452–2456.

(26) De Weerd, C.; Gomez, L.; Zhang, H.; Buma, W. J.; Nedelcu, G.; Kovalenko, M. V.; Gregorkiewicz, T. *J. Phys. Chem. C* **2016**, *120*, 13310–13315.

(27) Rowland, C. E.; Fedin, I.; Zhang, H.; Gray, S. K.; Govorov, A. O.; Talapin, D. V.; Schaller, R. D. *Nat. Mater.* **2015**, *14*, 484–489.

(28) Marcus, R. A. *Annu. Rev. Phys. Chem.* **1964**, *15*, 155–196.

(29) Huang, J.; Stockwell, D.; Huang, Z.; Mohler, D. L.; Lian, T. *J. Am. Chem. Soc.* **2008**, *130*, 5632–5633.

(30) El-Ballouli, A. O.; Alarousu, E.; Bernardi, M.; Aly, S. M.; Lagrow, A. P.; Bakr, O. M.; Mohammed, O. F. *J. Am. Chem. Soc.* **2014**, *136*, 6952–6959.

(31) Zhu, H.; Yang, Y.; Hyeon-Deuk, K.; Califano, M.; Song, N.; Wang, Y.; Zhang, W.; Prezhdo, O. V.; Lian, T. *Nano Lett.* **2014**, *14*, 1263–1269.

(32) Olshansky, J. H.; Ding, T. X.; Lee, Y. V.; Leone, S. R.; Alivisatos, A. P. *J. Am. Chem. Soc.* **2015**, *137*, 15567–15575.

(33) Zhu, H.; Yang, Y.; Wu, K.; Lian, T. *Annu. Rev. Phys. Chem.* **2016**, *67*, 259–281.

(34) Hyeon-Deuk, K.; Kim, J.; Prezhdo, O. V. *J. Phys. Chem. Lett.* **2015**, *6*, 244–249.

(35) Graff, B. M.; Bloom, B. P.; Wierzbinski, E.; Waldeck, D. H. *J. Am. Chem. Soc.* **2016**, *138*, 13260–13270.

(36) Diroll, B. T.; Fedin, I.; Darancet, P.; Talapin, D. V.; Schaller, R. D. *J. Am. Chem. Soc.* **2016**, *138*, 11109–11112.

(37) Bridewell, V. L.; Alam, R.; Karwacki, C. J.; Kamat, P. V. *Chem. Mater.* **2015**, *27*, 5064–5071.

(38) Yang, Y. A.; Wu, H.; Williams, K. R.; Cao, Y. C. *Angew. Chemie - Int. Ed.* **2005**, *44*, 6712–6715.

(39) Protesescu, L.; Yakunin, S.; Bodnarchuk, M. I.; Krieg, F.; Caputo, R.; Hendon, C. H.; Yang, R. X.; Walsh, A.; Kovalenko, M. V. *Nano Lett.* **2015**, *15*, 3692–3696.

(40) Shevchenko, E. V; Talapin, D. V; Kotov, N. A.; Brien, S. O.; Murray, C. B. *Nature* **2006**, *439*, 55–59.

(41) Overgaag, K.; Evers, W.; De Nijs, B.; Koole, R.; Meeldijk, J.; Vanmaekelbergh, D. *J. Am. Chem. Soc.* **2008**, *130*, 7833–7835.

(42) Chen, Z.; Moore, J.; Radtke, G.; Sirringhaus, H.; O'Brien, S. *J. Am. Chem. Soc.* **2007**, *129*, 15702–15709.

(43) Ravi, V. K.; Markad, G. B.; Nag, A. *ACS Energy Lett.* **2016**, *1*, 665–671.

(44) Spittel, D.; Poppe, J.; Meerbach, C.; Ziegler, C.; Hickey, S. G.; Eychmüller, A. *ACS Nano* **2017**, *11*, 12174–12184.

(45) Li, Q.; Lian, T. *Nano Lett.* **2017**, *17*, 3152–3158.

(46) Hunsche, S.; Dekorsy, T.; Klimov, V.; Kurz, H. *Appl. Phys. B* **1996**, *62*, 3–10.

(47) Infelta, P. P.; Gratzel, M.; Thomas, J. K. *J. Phys. Chem.* **1974**, *78*, 190–195.

For Table of Contents Only